European Journal of Chemistry

Check for updates

View Journal Online
View Article Online

Pharmaceutical organic salt: Disordered crystal structure of levofloxacin with γ-resorcylic acid

Syed Muddassir Ali Mashhadi [1,2,*], Muhammad Nawaz Tahir [3], David Apperley [4], Moazzam Hussain Bhatti [1], Muhammad Ashfaq [3,5] and Uzma Yunus [1,*]

[1] *Department of Chemistry, Allama Iqbal Open University, Islamabad, 44310, Pakistan*
muddassir_bakie@yahoo.com (S.M.A.M.), moazzamhussain_b@yahoo.com (M.H.B.), uzma_yunus@yahoo.com (U.Y.)
[2] *Department of Chemistry, University of Agriculture Faisalabad (Depalpur Okara Campus), Okara, 56130, Pakistan*
[3] *Department of Physics, University of Sargodha, Sargodha, 40100, Pakistan*
dmntahir_uos@yahoo.com (M.N.T.), muhammadashfaq1400@gmail.com (M.A.)
[4] *Department of Chemistry, Durham University, Stockton Road, Durham, DH1 3LE, United Kingdom*
d.c.apperley@durham.ac.uk (D.A.)
[5] *Department of Physics, University of Mianwali, Mianwali, 42200, Pakistan*

* *Corresponding author at: Department of Chemistry, Allama Iqbal Open University, Islamabad, 44310, Pakistan.*
e-mail: muddassir_bakie@yahoo.com (S.M.A. Mashhadi); uzma_yunus@yahoo.com (U. Yunus).

RESEARCH ARTICLE

10.5155/eurjchem.12.3.323-328.2134

Received: 06 July 2021
Received in revised form: 02 August 2021
Accepted: 08 August 2021
Published online: 30 September 2021
Printed: 30 September 2021

KEYWORDS

SC-XRD
SS-NMR
Organic salt
Levofloxacin
γ-Resorcylic acid
Disordered crystal structure

ABSTRACT

This study reports an organic salt prepared from an antibacterial drug, levofloxacin and antioxidant γ-resorcylic acid. A simple preparation method leads to a crystal with disordered structure. The idea is to prepare an organic salt comprising of pharmaceutically acceptable acidic and basic components. The salt is characterised by IR, solid state NMR, and single crystal XRD. Crystal data for $C_{25}H_{26}N_3O_8F$: triclinic, space group *P*-1 (no. 2), a = 7.0037(8) Å, b = 12.764(3) Å, c = 13.909(3) Å, α = 104.821(4)°, β = 92.039(4)°, γ = 95.334(4)°, V = 1194.6(4) Å^3, Z = 2, T = 296(2) K, μ(MoKα) = 0.113 mm^{-1}, *Dcalc* = 1.433 g/cm^3, 16879 reflections measured (5.048° ≤ 2Θ ≤ 54.186°), 5139 unique (R_{int} = 0.0663, R_{sigma} = 0.0975) which were used in all calculations. The final R_1 was 0.1121 (I>2σ(I)) and wR_2 was 0.2505 (all data). SC-XRD analysis shows that the crystal packing is stabilized by strong H-bonding of type N-H···O and comparatively weak interactions of type C-H···O, C-H···π and off-set π···π stacking.

Cite this: *Eur. J. Chem.* **2021**, *12(3)*, 323-328 **Journal website**: www.eurjchem.com

1. Introduction

Multicomponent crystals [1], such as salts, cocrystals [2-5], and solvates / hydrates, play a key role in the design of novel solid forms, especially in the pharmaceutical arena. Solid forms display exclusive physicochemical properties influencing key features of the formulated API like bioavailability, stability, flowability and manufacturability [6]. About 50% of marketed drugs are in salt form consisting stoichiometric ratio of anion and cation keeping in view of the higher bioavailability associated with them [7]. Generally, for complementary ions a p*K*a difference of ≥3 is expected for formation of salts [8], however it is not a universal truth applicable to salt formation. Improvement of dissolution, stability, hygroscopicity, and solubility profile can be achieved, which makes salt selection a multi-dimensional approach. Pharmaceutical organic salt [9,10] is an important solid-state form of drugs having impact during drug development process.

Levofloxacin (LEV), the levo isomer of ofloxacin, is a third generation fluoroquinolone that is used as a broad-spectrum antibiotic for various Gram-positive and Gram-negative organisms [11] and some other pathogens such as Mycoplasma, Chlamydia, Legionella, and Myobacteria spp. [12] are also used for the treatment of chronic bronchitis as well as urinary tract, kidney and skin infections [13] in patients with severe pneumonia and legionnaires disease levofloxacin exerted superior activity [13]. LEV is slightly water soluble having unpleasant taste and keeping in view of its lower solubility it is administered as a hydrochloride salt. It is absorbed from the gastrointestinal tract and the peak plasma concentration is reached in 1 to 2 hours after oral intake. Pharmacokinetically, LEV shows high bioavailability, low protein binding (30-40%), high tissue concentrations, and elimination via the kidneys with negligible liver metabolism.

ISSN 2153-2249 (Print) / ISSN 2153-2257 (Online)
https://dx.doi.org/10.5155/eurjchem.12.3.323-328.2134

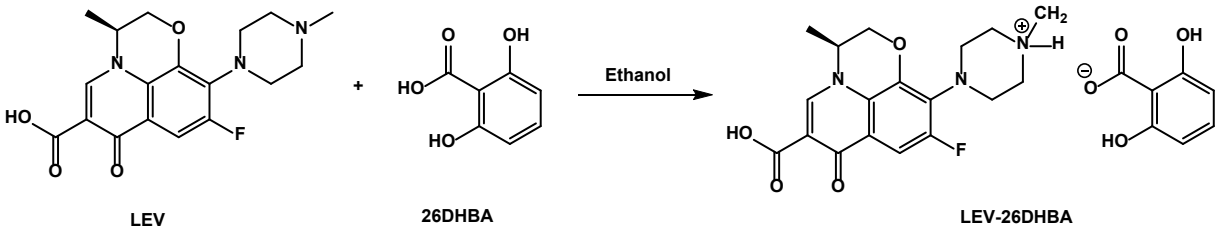

Scheme 1. Preparation of LEV-26DHBA.

γ-Resorcylic acid, also called 2,6-dihydroxybenzoic acid (26DHBA), is one of the strongest carboxylic acids [14] that has intramolecular hydrogen bonding. It is secondary metabolite of salicylic acid which is hydrolysed by liver enzymes. As 26DHBA is not a hazardous substance or generally regarded as safe (GRAS) compound according to regulations and its acidity makes it ideal for organic salt preparation.

In this study we report development (Scheme 1) and structure elucidation of an organic salt of LEV with pKa = 6.2 and 26DHBA having p*K*a = 1.3. prepared organic salt 4-(6-carboxy-9-fluoro-3-methyl-7-oxo-2,3-dihydro-7*H*-[1,4]oxazino [2,3,4-ij]quinolin -10-yl)-1-methylpiperazin-1-ium 2,6-dihydroxybenzoate (LEV-26DHBA) comprises of an antibacterial and an antioxidant GRAS component with the disordered crystal structure.

2. Experimental

2.1. Instrumentation

The Infrared spectra were recorded on Varian 640-IR spectrophotometer in ATR mode. Solid-state ^{13}C NMR spectra were recorded on a Bruker Avance III HD spectrometer with a ^{13}C resonant frequency of 125.7 MHz at a magnetic field strength of 11.7 T. 100 mg of crystalline sample was packed into a 4-mm rotor made up of zirconia equipped with a Kel-F cap. Spectral acquisition was done by the cross-polarization magic angle spinning (CP-MAS) pulse sequence at a spinning rate of 10.00 kHz. Magic angle calibration was done using KBr. Spectra were obtained using a relaxation delay of 4 seconds for LEV and LEV-26DHBA, while the same was 300 seconds for 26DHBA. Number of scans were 12800 for LEV, 1480 for LEV-26DHBA and 24 for 26DHBA. Data sets were Fourier transformed with a 5 Hz line broadening factor and phase corrected to produce a frequency domain spectrum. The chemical shifts were referenced indirectly to neat tetramethyl silane by setting the high frequency signal of adamantane to 38.5 ppm. Single crystal X-ray data was collected using a Bruker Kappa APEX II CCD diffractometer equipped with a graphite monochromator at 296 K. A fine focus of MoKα tube was used. Data were collected using APEX2 software, SAINT, for indexing the reflections and determining the unit cell parameters. The structure was solved by direct methods using SHELXS-97 software and refined by full-matrix least square calculations using SHELXL-2018/3 software. Crystallographic data for the structure has been deposited with the Cambridge Crystallographic Data Centre with CCDC deposition number 1976923. PLATON and Mercury 4.2 are utilized for the graphical representation of SC-XRD results.

2.2. Preparation of LEV-26DHBA

Isoniazid was received as a gift and other chemicals were purchased from Merck and were used as received from the supplier without any further purification. LEV and 26DHBA were separately dissolved in ethanol by sonication for 3 minutes, both equimolar (1 millimolar) solutions were mixed after heating at 45 °C. A white solid was formed when the two solutions were mixed (nearly all of the reacting material gave the product). Solid-state NMR suggested the product formation. Good crystals for the single-crystal XRD experiment were grown by dissolving the coformers in large amounts of solvent which were mixed and placed for slow evaporation of the solvent. White crystals were formed after seven days.

3. Result and discussion

3.1. Characterization

The IR spectra of LEV-26DHB revealed that the characteristic aromatic ring peaks, cyclic ketone, and amine groups are retained in the compound. The O-H stretch peak is present at 3065 cm^{-1}. Carboxylate anion (–COO–) formation due to salt formation which shows a single stretch at 1232 cm^{-1} [15]. Stretch at 1089 cm^{-1} is due to the presence of fluorine. An asymmetric stretch at 1619 cm^{-1} and symmetric stretch at 1450 cm^{-1} are identified for amine salts. The ammine stretch is present at 3479 cm^{-1}. The peak at 1713 cm^{-1} is due to the stretching of the carbonyl group.

Figure 1 shows the carbon-13 solid-state NMR spectra of the product and the coformers. The spectrum of the product is clearly distinguishable from the starting materials. There is no evidence for a significant contribution to the product spectrum from either of the starting materials (although it should be noted that it would be difficult to detect the 26DHBA component under the experimental conditions used to obtain the spectrum from the product). Several resonances between δ 120 and 140 ppm in the spectrum of the product appear in pairs. These are most likely to be associated with the LEV component of the product. This is consistent with the disorder over the two sites detected in the XRD measurement.

3.2. Single crystal structure

In LEV-26DHBA (Figure 2, Table 1) some parts of both cation and anion are disordered over two sets of sites with occupancy ratio of 0.541(12):0.459(12). Some important bond lengths and bond angles are given in Tables 2 and 3. In the cation, the 4-(6-carboxy-9-fluoro-3-methyl-7-oxo-2,3-dihydro-7*H*-[1, 4] oxazino[2,3,4-ij]quinolin-10-yl) part is disordered, A (C1-C10/C11A/C12A/C13A/N1/O1-O4/F1) and B (C1-C10/C11B/C12B/C13B/N1/O1-O4/F1) are roughly planar with RMS deviations of 0.1412 and 0.1396 Å, respectively.

The piperazine group is in the chair conformation with the basal plane C (C14-C17) [RMS deviation 0.0063 Å] and the apical atoms N2 and N3 at a distance of -0.664(9) and 0.630(9) Å, respectively. This major difference is due to the attached methyl group at N3 and the hydrogen coming from the carboxyl group of 26DHBA.

The dihedral angle between A/B, A/C, and B/C is 1.668(17), 56.62(22) and 57.92(22)°, respectively. In the anion 2,6-dihydroxybenzoate, the dihydroxybenzene is disordered with major and minor parts D (C20A-C25A/O7A/O8A) [RMS deviation 0.0635 Å] and E (C20B-C25B/O7B/O8B) [RMS deviation 0.0814 Å].

Table 1. Crystal data and structure refinement for LEV-26DHBA PUB.

Empirical formula	$C_{25}H_{26}N_3O_8F$
Formula weight	515.49
Temperature (K)	296(2)
Crystal system	Triclinic
Space group	*P*-1
a, (Å)	7.0037(8)
b, (Å)	12.764(3)
c, (Å)	13.909(3)
α (°)	104.821(4)
β (°)	92.039(4)
γ (°)	95.334(4)
Volume (Å^3)	1194.6(4)
Z	2
ρ_{calc} (g/cm^3)	1.433
μ (mm^{-1})	0.113
F(000)	540.0
Crystal size (mm^3)	0.40 × 0.22 × 0.18
Radiation	MoKα (λ = 0.71073)
2Θ range for data collection (°)	5.048 to 54.186
Index ranges	$-8 \le h \le 7, -16 \le k \le 16, -17 \le l \le 17$
Reflections collected	16879
Independent reflections	5139 [R_{int} = 0.0663, R_{sigma} = 0.0975]
Data/restraints/parameters	5139/14/303
Goodness-of-fit on F^2	1.039
Final *R* indexes [I≥2σ (I)]	R_1 = 0.1121, wR_2 = 0.2189
Final *R* indexes [all data]	R_1 = 0.2040, wR_2 = 0.2505
Largest diff. peak/hole (e Å^{-3})	0.35/-0.39
CCDC number	1976923

Table 2. Bond lengths for LEV-26DHBA.

Atom	Atom	Length (Å)	Atom	Atom	Length (Å)
F1	C8	1.362(6)	C11A	C12A	1.506(15)
O1	C1	1.330(7)	C12A	C13A	1.512(15)
O2	C1	1.199(7)	C11B	C12B	1.485(17)
O3	C3	1.270(6)	C12B	C13B	1.516(17)
O4	C11A	1.365(12)	C14	C15	1.503(8)
O4	C10	1.368(6)	C16	C17	1.500(8)
O4	C11B	1.408(13)	O5	C19	1.286(9)
N1	C6	1.340(7)	O6	C19	1.246(9)
N1	C5	1.404(7)	C19	C20B	1.441(12)
N1	C12B	1.494(13)	C19	C20A	1.522(11)
N1	C12A	1.501(12)	O7A	C21A	1.352(12)
N2	C9	1.393(7)	O8A	C25A	1.318(11)
N2	C17	1.445(7)	C20A	C21A	1.3900
N2	C14	1.458(7)	C20A	C25A	1.3900
N3	C15	1.481(8)	C21A	C22A	1.3900
N3	C16	1.487(7)	C22A	C23A	1.3900
N3	C18	1.488(7)	C23A	C24A	1.3900
C1	C2	1.485(8)	C24A	C25A	1.3900
C2	C6	1.350(8)	O7B	C21B	1.347(13)
C2	C3	1.434(8)	O8B	C25B	1.384(13)
C3	C4	1.442(7)	C20B	C21B	1.3900
C4	C5	1.405(7)	C20B	C25B	1.3900
C4	C7	1.416(8)	C21B	C22B	1.3900
C5	C10	1.397(7)	C22B	C23B	1.3900
C7	C8	1.337(8)	C23B	C24B	1.3900
C8	C9	1.410(8)	C24B	C25B	1.3900
C9	C10	1.399(8)			

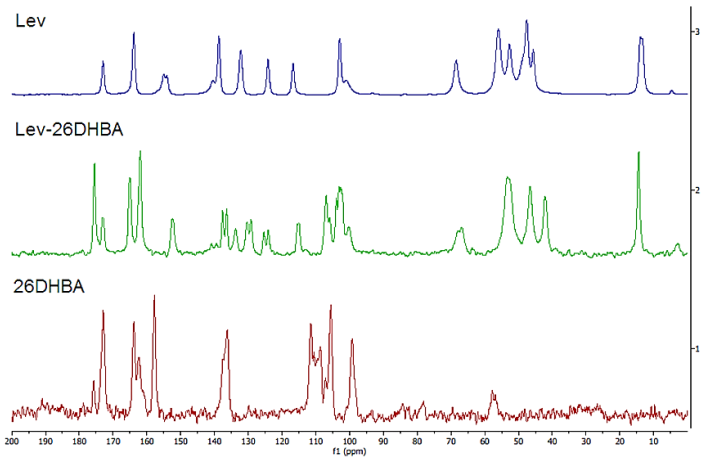

Figure 1. ^{13}C solid state NMR spectrum of LEV-26DHBA.

Table 3. Bond Angles for LEV-26DHBA.

Atom	Atom	Atom	Angle (°)	Atom	Atom	Atom	Angle (°)
C11A	O4	C10	115.7(8)	N1	C12A	C11A	107.8(11)
C10	O4	C11B	114.9(8)	N1	C12A	C13A	113.0(13)
C6	N1	C5	118.4(5)	C11A	C12A	C13A	107.3(13)
C6	N1	C12B	121.5(6)	O4	C11B	C12B	118.4(13)
C5	N1	C12B	117.4(6)	C11B	C12B	N1	102.0(13)
C6	N1	C12A	121.9(6)	C11B	C12B	C13B	109.3(16)
C5	N1	C12A	118.6(6)	N1	C12B	C13B	108.3(13)
C9	N2	C17	124.4(5)	N2	C14	C15	109.2(5)
C9	N2	C14	122.2(5)	N3	C15	C14	110.5(5)
C17	N2	C14	112.0(5)	N3	C16	C17	110.8(5)
C15	N3	C16	111.7(5)	N2	C17	C16	110.0(5)
C15	N3	C18	112.1(5)	O6	C19	O5	121.9(8)
C16	N3	C18	111.3(5)	O6	C19	C20B	120.5(11)
O2	C1	O1	121.1(6)	O5	C19	C20B	117.5(11)
O2	C1	C2	124.2(6)	O6	C19	C20A	121.8(9)
O1	C1	C2	114.6(6)	O5	C19	C20A	116.3(10)
C6	C2	C3	119.4(5)	C21A	C20A	C25A	120.0
C6	C2	C1	118.2(5)	C21A	C20A	C19	122.7(11)
C3	C2	C1	122.5(5)	C25A	C20A	C19	116.9(11)
O3	C3	C2	122.4(5)	O7A	C21A	C20A	118.8(10)
O3	C3	C4	121.4(5)	O7A	C21A	C22A	120.9(10)
C2	C3	C4	116.1(5)	C20A	C21A	C22A	120.0
C5	C4	C7	118.2(5)	C21A	C22A	C23A	120.0
C5	C4	C3	121.0(5)	C24A	C23A	C22A	120.0
C7	C4	C3	120.8(5)	C25A	C24A	C23A	120.0
C10	C5	N1	119.9(5)	O8A	C25A	C24A	110.4(12)
C10	C5	C4	120.6(5)	O8A	C25A	C20A	128.6(12)
N1	C5	C4	119.5(5)	C24A	C25A	C20A	120.0
N1	C6	C2	125.6(6)	C21B	C20B	C25B	120.0
C8	C7	C4	119.2(6)	C21B	C20B	C19	115.1(13)
C7	C8	F1	118.9(6)	C25B	C20B	C19	124.8(13)
C7	C8	C9	125.1(5)	O7B	C21B	C20B	123.4(12)
F1	C8	C9	115.9(5)	O7B	C21B	C22B	115.2(12)
N2	C9	C10	122.2(5)	C20B	C21B	C22B	120.0
N2	C9	C8	122.2(5)	C21B	C22B	C23B	120.0
C10	C9	C8	115.6(5)	C24B	C23B	C22B	120.0
O4	C10	C5	121.0(5)	C23B	C24B	C25B	120.0
O4	C10	C9	117.9(5)	O8B	C25B	C24B	123.8(14)
C5	C10	C9	121.1(5)	O8B	C25B	C20B	115.7(14)
O4	C11A	C12A	115.2(10)	C24B	C25B	C20B	120.0

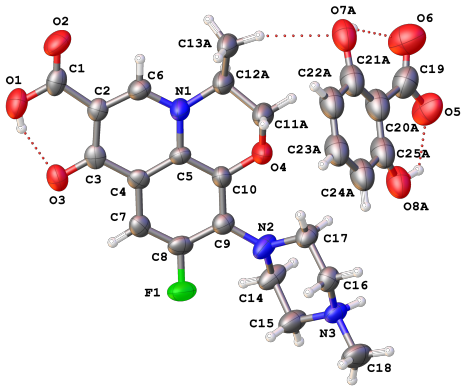

Figure 2. ORTEP diagram of LEV-26DHBA drawn at a probability level of 50%. H-atoms are shown by small circles of arbitrary radius. Only the major part of the disordered groups are shown for clarity.

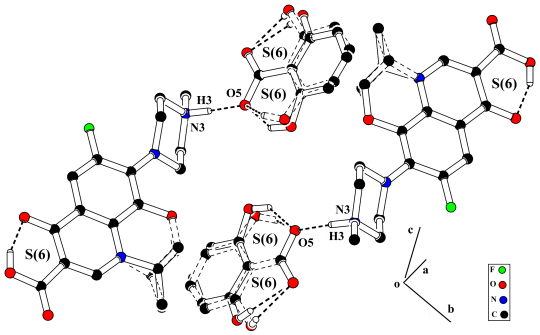

Figure 3. Packing diagram of LEV-26DHBA showing intramolecular H-bonding and strong intermolecular H-bonding. Selected H-atoms are shown for clarity.

Table 4. Hydrogen bond geometry and C-H···π interaction for LEV-26DHBA.

D	H	A	d(D-H) (Å)	d(H-A) (Å)	d(D-A) (Å)	D-H-A (°)
O1	H1	O3	0.82	1.80	2.548(6)	150.7
N3	H3	O5[1]	0.93(6)	1.76(6)	2.633(7)	156(6)
C13A	H13B	O6[2]	0.96	2.64	3.588(17)	170.1
C13A	H13C	O7A	0.96	2.58	3.50(2)	159.0
C11B	H11C	O3[3]	0.97	2.53	3.392(19)	147.5
C12B	H12B	O3[4]	0.98	2.61	3.461(18)	144.7
C14	H14B	F1	0.97	2.28	2.825(8)	114.9
C14	H14B	O2[3]	0.97	2.64	3.289(7)	124.7
C16	H16A	O8B[5]	0.97	2.63	3.513(16)	152.0
C18	H18A	F1[6]	0.96	2.60	3.183(8)	119.7
C18	H18C	O2[7]	0.96	2.56	3.432(9)	151.5
O7A	H7A	O6	0.82	1.99	2.657(12)	137.6
O8A	H8A	O5	0.82	1.93	2.570(18)	134.1
C24A	H24A	O8A[5]	0.93	2.60	3.383(19)	142.7
O8B	H8B	O5	0.82	1.92	2.48(2)	124.7
C	**H**	***π***	**d(C-H) (Å)**	**d(C-π) (Å)**	**d(C-π) (Å)**	**C-H-π (°)**
C18	H18B	Cg1[8]	0.96	2.76	3.665 (10)	157

Symmetry codes: [1] 2-*x*, 1-*y*, 1-*z*; [2] 2-*x*, 1-*y*, -*z*; [3] 2-*x*, -*y*, -*z*; [4] 1-*x*, -*y*, -*z*; [5] 1-*x*, 1-*y*, 1-*z*; [6] 1-*x*, -*y*, 1-*z*; [7] +*x*, +*y*, 1+*z*, [8] -*x*+1, -*y*+1, -*z*+1. Cg1 is the centroid of the phenyl ring (C20A-C25A).

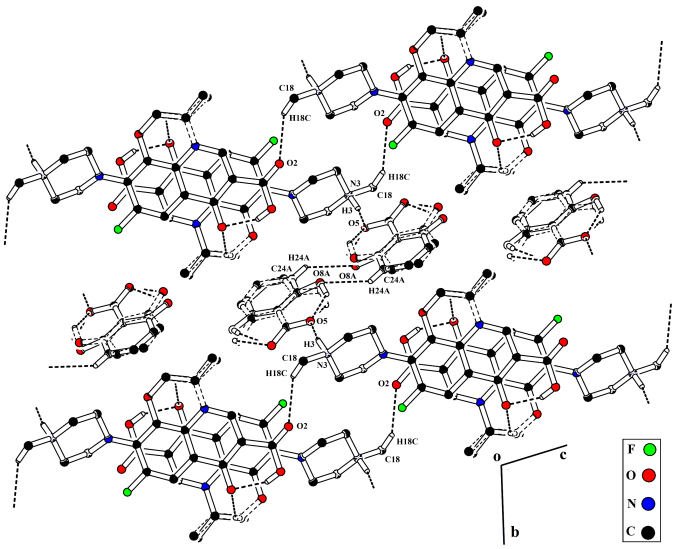

Figure 4. Packing diagram of LEV-26DHBA showing strong as well as weak H-bonding. Selected H-atoms are shown for clarity.

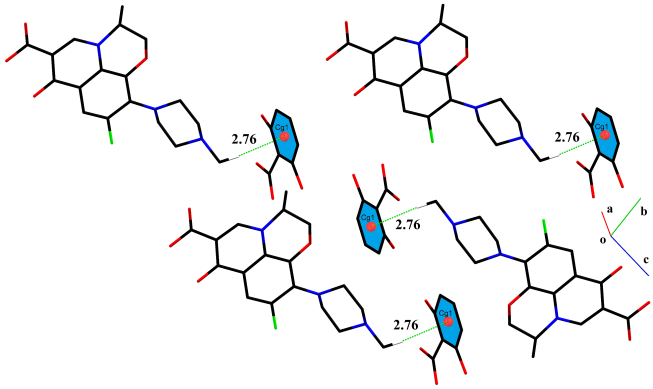

Figure 5. Graphical representation of C-H···π interaction in the crystal packing of LEV-26DHBA. Selected H-atoms are shown for clarity.

The carboxylate group F (C19/O5/O6) is, of course, planar. The dihedral angle between D/E, D/F, and E/F is 11.8(9), 9.75(1.28), and 3.72(1.52)°, respectively. This shows that the 2,6-dihydroxybenzoate molecules of the minor part are more planar as compared to the major part. Due to strong H-bonding, there exist two *S*(6) loops in the anion part and one in the cation part due to O-H···O bonding, also the cation and anion are linked by the strong H-bonding of N-H···O interaction (Figure 3). The weaker H-bonding joins the anions like dimmers due to C-H···O interactions with $R_2^2(8)$ loops (Figure 4). Furthermore, the C-H···O interaction between the H-atom of methyl at N3 and O-atom of the carbonyl group present in the cations link themselves in pairs. In this way, the molecules are mainly stabilized because of these hydrogen bonding.

In addition to H-bonding, comparatively weak interactions of type C-H···π and off-set π···π stacking helps in the further stabilization of the crystal packing. C-H···π interaction interlinked cation with anion with H···π distance of 2.76 Å as displayed in Figure 5 and given in Table 4. Off-set π···π stacking interaction is found between the phenyl rings of cations. This

interaction interlinked the cations with each other along a crystallographic axis (Figure 6). The centroid to centroid separation ranges from 3.72 to 3.87 Å, while the ring offset ranges from 1.31 to 1.64 Å.

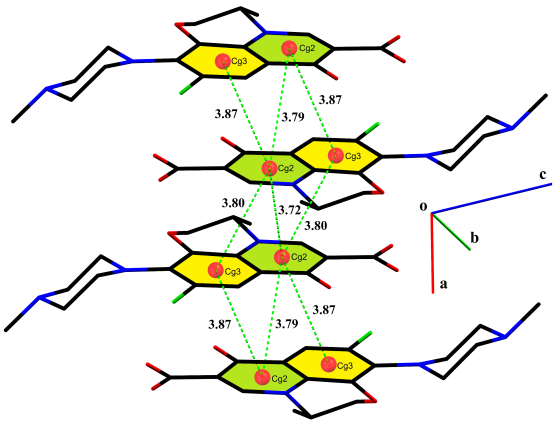

Figure 6. Graphical representation of off-set π···π stacking interaction in LEV-26DHBA. Anions and H-atoms are not shown for clarity.

4. Conclusion

The present study is the preparation and characterization of a pharmaceutical organic salt of LEV and 26DHBA. Crystal structure is characterized by IR, solid state NMR and single crystal XRD. Splitting of peaks in the solid-state NMR spectrum and single-crystal XRD results concluded that the crystal is disordered. Single-crystal XRD infers that the crystal packing is mainly stabilized by strong N-H···O bonding and further stabilization in the crystal packing is due to C-H···O, C-H···π and off-set π···π stacking interactions. This multicomponent salt comprises of antibacterial drug and a GRAS antioxidant component. This combination of two pharmaceutically acceptable components in single crystalline form may be administered to the patients who require both antibacterial Levofloxacin and antioxidants.

Acknowledgement

We are thankful to HEC Pakistan for providing funding for the characterization. We are also thankful to Dr. Paul Hodgkinson (Durham University) for valuable suggestions during ^{13}C and ^{1}H NMR experiments.

Supporting information

CCDC-1976923 contains the supplementary crystallographic data for this paper. These data can be obtained free of charge via www.ccdc.cam.ac.uk/data_request/cif, or by e-mailing data_request@ccdc.cam.ac.uk, or by contacting The Cambridge Crystallographic Data Centre, 12 Union Road, Cambridge CB2 1EZ, UK; fax: +44(0)1223-336033.

Disclosure statement

Conflict of interests: The authors declare that they have no conflict of interest.
Author contributions: All authors contributed equally to this work.
Ethical approval: All ethical guidelines have been adhered.
Sample availability: Samples of the compounds are available from the author.

ORCID

Syed Muddassir Ali Mashhadi
https://orcid.org/0000-0002-6455-7604
Muhammad Nawaz Tahir
https://orcid.org/0000-0002-6815-9806
David Apperley
https://orcid.org/0000-0001-7102-0314
Moazzam Hussain Bhatti
https://orcid.org/0000-0003-4868-6032
Muhammad Ashfaq
https://orcid.org/0000-0001-6663-8777
Uzma Yunus
https://orcid.org/0000-0002-8261-0595

References

[1]. Mashhadi, S. M. A.; Yunus, U.; Bhatti, M. H.; Ahmed, I.; Tahir, M. N. *J. Mol. Struct.* **2016**, *1117*, 17–21.
[2]. Mashhadi, S. M. A.; Yunus, U.; Bhatti, M. H. *J. Mol. Struct.* **2021**, *1233* (130015), 130015.
[3]. Mashhadi, S. M. A.; Yunus, U.; Bhatti, M. H.; Tahir, M. N. *J. Mol. Struct.* **2014**, *1076*, 446–452.
[4]. Mashhadi, S. M. A.; Batsanov, A. S.; Sajjad, S. A.; Nazir, Y.; Bhatti, M. H.; Yunus, U. *J. Mol. Struct.* **2021**, *1226* (129388), 129388.
[5]. Mashhadi, S. M. A.; Yufit, D.; Liu, H.; Hodgkinson, P.; Yunus, U. *J. Mol. Struct.* **2020**, *1219* (128621), 128621.
[6]. Lehn, J.-M. *Science* **2002**, *295* (5564), 2400–2403.
[7]. Cram, D. J. *Angew. Chem. Int. Ed. Engl.* **1988**, *27* (8), 1009–1020.
[8]. Cram, D. J.; Cram, J. M. *Acc. Chem. Res.* **1978**, *11* (1), 8–14.
[9]. Carvalho, P. S.; Diniz, L. F.; Tenorio, J. C.; Souza, M. S.; Franco, C. H. J.; Rial, R. C.; Warszawski de Oliveira, K. R.; Nazario, C. E. D.; Ellena, J. *CrystEngComm* **2019**, *21* (24), 3668–3678.
[10]. Odiase, I.; Nicholson, C. E.; Ahmad, R.; Cooper, J.; Yufit, D. S.; Cooper, S. J. *Acta Crystallogr. C Struct. Chem.* **2015**, *71* (Pt 4), 276–283.
[11]. Tasso, L.; de Andrade, C.; Dalla Costa, T. *Int. J. Antimicrob. Agents* **2011**, *38* (4), 307–313.
[12]. Fish, D. N.; Chow, A. T. *Clin. Pharmacokinet.* **1997**, *32* (2), 101–119.
[13]. Blázquez Garrido, R. M.; Espinosa Parra, F. J.; Alemany Francés, L.; Ramos Guevara, R. M.; Sánchez-Nieto, J. M.; Segovia Hernández, M.; Serrano Martínez, J. A.; Huerta, F. H. *Clin. Infect. Dis.* **2005**, *40* (6), 800–806.
[14]. Gdaniec, M.; Gilski, M.; Denisov, G. S. *Acta Crystallogr. C* **1994**, *50* (10), 1622–1626.
[15]. Bandari, S.; Dronam, V. R.; Eedara, B. B. *J. Pharm. Investig.* **2017**, *47* (6), 583–591.